Available online at www.sciencedirect.com
SCIENCE DIRECT
Medical Engineering & Physics 27 (2005) 810–826
Medical Engineering & Physics
www.elsevier.com/locate/medengphy

Review

The role of computational models in the search for the mechanical behavior and damage mechanisms of articular cartilage

W. Wilson, C.C. van Donkelaar *, R. van Rietbergen, R. Huiskes

Department of Biomedical Engineering, Eindhoven University of Technology, P.O. Box 513, Eindhoven 5600 MB, The Netherlands

Received 1 October 2004; received in revised form 8 February 2005; accepted 11 March 2005

Abstract

Articular cartilage plays a vital role in the function of diarthrodial joints. Due to osteoarthritis degeneration of articular cartilage occurs. The initial event that triggers the pathological process of cartilage degeneration is still unknown. Cartilage damage due to osteoarthritis is believed to be mechanically induced. Hence, to investigate the initiation of osteoarthritis the stresses and strains in the cartilage must be determined. So far the most common method to accomplish that is finite element analysis. This paper provides an overview of computational descriptions developed for this purpose, and what they can be used for. Articular cartilage composition and structure are discussed in relation with degenerative changes, and how these affect mechanical properties.

Keywords: Cartilage; Finite element analysis; Damage; Collagen; Swelling

Contents

Abbreviations: AC, articular cartilage; AGE, advanced glycation end product; FCD, fixed charge density; FEA, finite element analysis; OA, osteoarthritis; PG, proteoglycan

* Corresponding author. Tel.: +31 40 247 3135; fax: +31 40 244 7355.
E-mail address: c.c.v.donkelaar@tue.nl (C.C. van Donkelaar).

1350-4533/$ – see front matter © 2005 IPEM. Published by Elsevier Ltd. All rights reserved.
doi:10.1016/j.medengphy.2005.03.004

1. Introduction

Articular cartilage (AC) covers the articulating ends of diarthrodial joints. It plays a vital role in the function of the musculoskeletal system by allowing almost frictionless motion to occur between the articular surfaces of a diarthrodial joint [1]. Furthermore, it distributes the loads over a large contact area, thereby minimizing the contact stress, and dissipates the energy associated with dynamic loads [2].

Osteoarthritis (OA), which involves degeneration of AC, is the most common cause of disability in elderly, with prevalence increasing with age. The overall prevalence for moderate to severe OA is approximately 20%. By the age of 55–65, up to 85% of all people will have some degree of OA in one or more joints. Pain and disability characterize the condition, and severe OA is the main reason for joint replacement surgery. According to Radin et al. [3] OA can be defined as mechanically induced thickness loss of AC, with thickening and eburnation of the underlying subchondral bone and, usually, a secondary inflammation of the synovium. It is generally assumed that OA is caused by mechanical overloading. Nonetheless, the initial event that triggers the pathological process of cartilage degeneration is still unknown.

As the main function of AC is load bearing, it is important to understand its mechanical behavior. In order to investigate the initiation of osteoarthritis the stresses and strains in the cartilage must be determined. So far the most common method to calculate stresses and strains in AC is finite element analysis (FEA).

In the literature many material models for AC can be found. These models range from relatively simple ones, including the biphasic nature of the AC, to models that include descriptions of all major individual components of AC. To validate these models, data from confined compression, unconfined compression, and indentation experiments are often used.

During each of these tests the load distribution between the different components within the tissue varies. Hence, from each of these tests different material properties can be derived. Most of the models available in the literature can account for one of these experiments, while others can account for multiple tests or all of them simultaneously. Generally speaking, the most realistic models are complex, and computationally expensive. Hence, one should always use the simplest model that is sufficient to obtain the required data.

This paper gives an overview of different material models developed for articular cartilage, and what they can be used for. To choose what kind of model one needs, knowledge of AC mechanical properties is helpful. Therefore, this paper starts with a review of composition and structure of AC, together with their changes during degeneration, and how they influence mechanical properties. Then an overview of AC computational descriptions currently available in the literature is given, followed by a discussion of their advantages and disadvantages.

2. Cartilage composition and structure

AC can be considered as a solid matrix, saturated with water and mobile ions. The solid matrix consists of cartilage cells (chondrocytes) embedded in an extracellular matrix. The major components of the extracellular matrix are collagen molecules and negatively charged proteoglycans (PGs) (Fig. 1). The material properties of cartilage depend primarily on the properties of the extracellular matrix. Composition, maintenance and gradual turnover of the matrix depend on the biosynthetic activity of chondrocytes [4].

2.1. Proteoglycans

PGs form approximately 30–35% of the dry tissue weight [5]. They are large, complex biomolecules composed of a central protein core with negatively charged glycoaminoglycans (GAG) side chains covalently attached [6]. These groups give rise to a high negative charge density, quantified as the

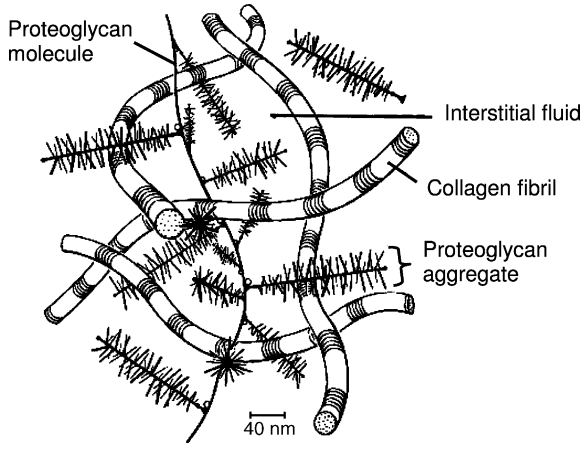

Fig. 1. Schematic depiction of cartilage structure (adapted from [188]).

fixed charged density (FCD) [4,7]. Due to the FCD, the cation concentration inside the tissue is higher than in the surrounding synovial fluid, which causes a pressure difference that results in swelling of the tissue [8].

2.2. Collagen

Collagen forms approximately 50–75% of dry tissue weight [5,9]. AC contains primarily type II collagen (80–85%), with smaller amounts of collagen types V, VI, IX, X, and XI [10,11]. Collagen molecules assemble to form small fibrils and larger fibers with an exquisite architectural arrangement and with dimensions that vary through the depth of the cartilage layer [12–15]. Collagen fibers do not offer significant resistance to pressures, but are stiff and strong in tension [16–19]. Hence, they provide resistance against swelling and tensile strains [20].

The stiffness of the collagen network is highly influenced by the amount of cross-links. Cross-links can be divided in two different categories of interaction, one involving physical entwinement which would not allow for network disconnection unless actual fibril breakage occurs [21], and the other based on some form of mediated or direct fibril-to-fibril interaction not involving entwinement [22] (Fig. 2). Results from structural [23,24], and ultrastructural [25] studies do not suggest a high entwinement density. Examples of cross-links that do not involve physical entwinement are those by collagen types IX and XI, by PGs and by advanced glycation end products (AGEs).

Type IX collagen, which is located at the exterior of the fibrils in an antiparallel orientation that follows a regular D-periodicity [26], appears to have an important role in stabilizing the three-dimensional organization of the collagen network [27,26,28]. It thus contributes to the ability of collagen to resist the swelling pressure caused by PGs and the tensile stresses developed within the tissue when loaded [29–32]. Collagen type XI, buried within the fibrils where it is covalently linked with collagen type II via hydroxylysine-based aldehyde cross-links [11], is believed to regulate fibril size [10,33].

The chondroitin 4/6-sulfate side chains of the PGs can electrostatically bind to the collagen fibrils, forming a cross-linked rigid matrix [34]. Therefore, the extracellular matrix of cartilage can be seen as a composite structure of collagen type II fibrils with intertwining proteoglycan aggregates [34].

AGEs are formed by nonenzymantic glycation of proteins, which is initiated by the reaction of sugars with lysine and arginine residues in proteins [35]. Generation of AGE crosslinking results in stiffening of the AC collagen network [35,36], which makes it more brittle [37]. In AC, increasing levels of AGEs are found with increasing age [38–40].

2.3. Chondrocytes

Chondrocytes are metabolically active cells responsible for the synthesis, incorporation, organization and degradation of matrix components [41]. Because chondrocytes lack direct cell-to-cell contact and cartilage also lacks blood and lymphatic vessels, chondrocytes receive nutrients from the synovial fluid via diffusion and/or convection through the matrix [4,42]. Changes in the environment through physical factors (e.g., stresses, strains, flow velocities, osmotic and hydraulic pressures, electric current and potentials), chemical factors

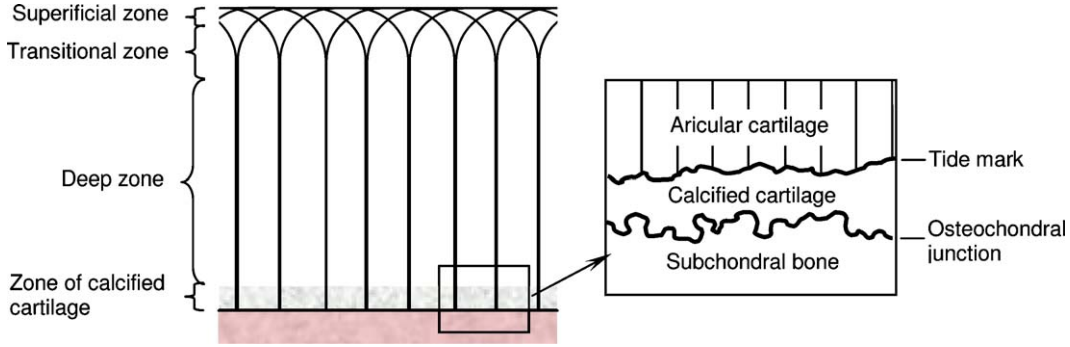

Fig. 2. Orientation of collagen fibers in different AC zones.

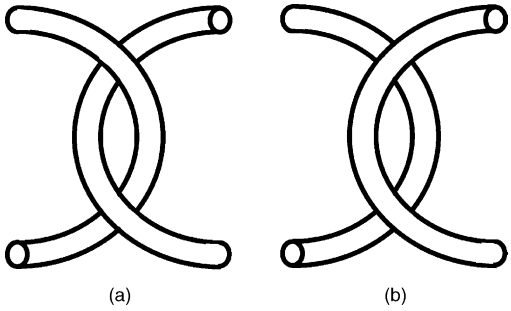

Fig. 3. Two schematic types of cross-linking created using (a) an entwinement based interaction, and (b) a nonentwinement based interaction (based on [22]).

(e.g., interleukins, growth factors, pharmaceutical agents) and matrix composition influence their synthetic response [43,44].

AC can be divided into four different layers, or zones (Fig. 3). From top to bottom these are the superficial, transitional, deep, and calcified cartilage zones.

2.4. Superficial zone

The superficial articular zone is the thinnest one and forms the gliding surface of the joint [5]. In this zone collagen and water content are highest (water content is approximately 85%) [7,45]. Collagen fibers are densely packed, have a small diameter, and are arranged parallel to the articular surface [15] (Fig. 3). The chondrocytes appear flattened and are relatively inactive [46]. Cell volume is smaller, cell density is higher and aggrecan content is lower in the superficial compared to the deeper zones [47,46]. PGs and collagen appear to be strongly interconnected in this zone, which may help the superficial zone to resist shear stresses produced by motion [9].

2.5. Transitional zone

The transitional zone occupies several times the volume of the superficial zone. The collagen fibers have a larger diameter and are more randomly arranged [15,11] (Fig. 3). The chondrocytes appear rounded and are larger and more active than in the superficial zone [5]. PG content is high in this zone and aggrecan aggregates are larger than in the superficial zone.

2.6. Deep zone

In the deep zone the collagen fibers have their largest diameters and are arranged perpendicular to the subchondral bone [15,48] (Fig. 3). This zone has a high PG content and the lowest water content (approximately 60%) [4]. The chondrocytes tend to be aligned in radial columns and the synthetic activity of the chondrocytes is highest [46,49,50].

2.7. Zone of calcified cartilage

The zone of calcified cartilage acts as a transition layer between bone and cartilage. The calcified zone is separated from the deep zone by an interface plane called the tidemark [11] (Fig. 3). The cartilage is mineralized (calcified) with crystals of calcium salts and has low PG content. The collagen fibers from the deep zone cross the tidemark and insert the calcified zone providing a strong anchoring system for the tissue on the subchondral bone [48,51]. The thickness of the calcified zone is a relatively constant percentage of the total cartilage thickness (approximately 5% with a range of 3–8%) [52]. This zone is calcified to the same extent as bone. Although less stiff than bone, the calcified zone is still 10–100 times stiffer than cartilage [53]. The tidemark and the junction between the zone of calcified cartilage and subchondral bone are both wavy (Fig. 3) and provide great resistance to shear stresses [54].

3. Relation between cartilage composition and its structural properties

From a mechanical point of view, the most relevant components of AC are the tight and highly organized collagen network together with the charged PG network. Below the relation between mechanical properties, composition and structure of the tissue are discussed.

3.1. Viscoelastic behavior

AC is highly viscoelastic. There are two distinct mechanisms responsible for this behavior [55–57]: (a) the frictional drag force of interstitial fluid flow through the porous solid matrix (i.e., the flow-dependent mechanism), and (b) the time-dependent deformability of the solid matrix (i.e., the flow-independent mechanism). Of the extracellular matrix both the collagen fibrils [58–64] and the PG gel in which they are embedded [65–67] have flow-independent viscoelasticity.

Due to exudation of fluid from the tissue when the cartilage is under load, a loss of tissue volume will occur. At equilibrium, no fluid flow or fluid pressure gradients exist, and the entire load is carried by the solid matrix and the internal swelling pressures. Upon removal of load or deformation, AC will recover to its initial dimensions, due to the elasticity of the solid matrix and the increased osmotic pressure within the tissue [68,69].

Fluid movement in loaded cartilage is governed by the hydraulic permeability of the solid matrix. Because the permeability of the extracellular matrix is relatively low, it is very difficult for the interstitial fluid to escape from the tissue under mechanical loading [70–73]. It was shown that the negative FCD of the PGs limit fluid flow, and thereby affect the permeability of the tissue [7,70,74,75]. The permeability is also highly dependent on pore sizes in the extracellular

matrix [68,69,74,75,76]. When the tissue is deformed both the FCD and pore sizes change [70,7,74,75]. Hence, the permeability of cartilage is strain-dependent.

3.2. Swelling behavior

The negatively charged groups of the PGs give rise to a high-net negative charge density that is quantified as the FCD [4,7]. In order for the cartilage to meet the electro-neutrality requirement, a large number of counter ions (e.g., Na^+) must be present within the interstitial matrix. The resulting ion concentration in the AC is therefore higher than in the surrounding synovial fluid. This excess of ion particles within the matrix creates a Donnan osmotic pressure difference between the internal and external environment of the tissue. Due to this pressure difference fluid will flow into the tissue to maintain osmotic equilibrium [8]. Another cause of swelling in AC is caused by repulsion of the closely spaced negatively charged groups of the PGs. This effect, called chemical expansion, also depends on the internal concentration of ions in the solution floating around the PGs, because these ions shield the charged groups somewhat from interacting with each other [77]. The collagen network prevents the tissue from swelling.

3.3. Compression behavior

The PGs are mainly responsible for the biomechanical characteristics in compression [4,67,78]. When the cartilage is loaded in compression, volumetric changes occur because of fluid movement within the tissue. With these volumetric changes the FCD inside the tissue increases, and thereby also the internal osmotic pressure and chemical expansion stress. Hence, the effective stiffness of the tissue increases with decreasing volume. As the collagen network prevents the swelling of the tissue, the swelling pressures in the tissue remain high. Through this mechanism the collagen fibrils also contributes to the compressive stiffness of AC.

3.4. Tensile behavior

The tensile modulus of AC depends on the collagen fibril density, fibril orientation and the amount of collagen cross-linking [16]. When cartilage is tested in tension, the collagen fibrils and entangled PG molecules are aligned and stretched along the axis of loading. For small deformations, when the tensile stress in the specimen is relatively small, a nonlinear toe-region is seen in the stress–strain curve, due to realignment of the collagen fibrils, rather than stretching of these fibers. For larger deformations, and after realignment, the collagen fibrils are stretched and therefore generate a larger tensile stress due to the intrinsic stiffness of the collagen fibrils themselves [18,19,79]. Due to this phenomenon the tensile stiffness of AC is highly strain-dependent. Due to the swelling pressures caused by the PGs the collagen network of AC is prestressed. Through this mechanism the PGs also influence the tensile stiffness of AC.

3.5. Shear behavior

Application of pure shear under small strains does (ideally) not cause volumetric changes of the tissue samples. Thus, no significant pressure gradient or fluid flow through the matrix should occur [67,80,81]. The intrinsic shear stiffness of the PG-collagen matrix is mainly associated with the collagen fibrils [67]. PGs by themselves may not contribute directly to the overall stiffness in shear. However, they prestress the collagen network because of their ability to generate swelling pressures [67].

3.6. Importance of inhomogeneity and anisotropy in the matrix components

Composition and structure of cartilage varies through the depth of the tissue. Hence, the mechanical properties of AC are nonhomogeneous and anisotropic. Due to the nonhomogeneous distribution of PGs, there is a nonhomogeneous distribution of FCD through the depth of the tissue [82,83,84], which results in depth-dependent swelling pressures.

As the orientation of the collagen fibers changes over the height of the tissue, and because they can only resist load in tension, the collagen network plays an important role in the mechanical inhomogeneity and anisotropy of AC. In the superficial zone the collagen fibrils are arranged parallel to the articular surface, thereby giving this layer a high tensile stiffness in this direction [18,19,85], while it has very low stiffness in the perpendicular direction. These fibrils therefore give a large contribution to the mechanical resistance against indentation, and hardly provide any resistance to swelling. The fibrils in the deeper zones are mainly oriented perpendicular to the articular surface, and therefore do provide great resistance against swelling.

4. Cartilage damage and degeneration

Mechanically, cartilage degeneration is characterized by an increase in thickness [86,87], decrease in stiffness [88], increase in permeability [11,88], and an increased water content [11,88,89,104,90,91]. In severely damaged cartilage cracks, initiate at the articular surface, and extend downwards at approximately 45° into the superficial [92,98], middle [92,93,98] and eventually deep zone [94,95]. Cracks along the tidemark [96–99] can emerge as well.

It is generally accepted that early cartilage degeneration due to OA is primarily related to changes in the PGs and in the collagen network [25,100–106]. However, the sequence and cause of the changes is unknown. The initially observed event of cartilage degeneration and OA is swelling of cartilage [76], which could result from damage to the strained collagen network, or from increased swelling as a result of an increased PG concentration. Both phenomena are known to occur in vivo.

4.1. Changes in the collagen network

Recently, strong indications were found that swelling after AC damage is caused by damage to the collagen network [107,108]. Several studies showed that fibrillation, clefts and disintegration of the collagenous fibril network in the transitional zone occur in early stages of cartilage degeneration [14,109–112]. Lewis and Johnson [113] found broken collagen fibrils at the tips of cracks, but most fibrils were partially peeled apart. This peeling process suggests that the fibrils are normally "tied" together in a parallel fashion [25,114,115], and that crack propagation starts by fibrils being peeled apart as a result of failure of the collagen fibril bonding [113]. The importance of interfibrillar bonding is also illustrated by McCormack and Mansour [116], who found that repeatedly indented samples were weaker in tension when loaded in the direction perpendicular to the radial fibrils, as compared to control samples, even though the superficial layer was still intact [117,118]. All these findings support the hypothesis of Clark and Simonian [106], which says (1) that the earliest change in the collagen matrix architecture is loosening of the cross-links between the large fibrils, which themselves remain intact until more severe degenerative changes occur, and (2) that this interfibrillar loosening mechanism initiates in the transitional zone of the cartilage, rather than at the surface.

4.2. Changes in PG content

During cartilage degeneration, PG content decreases due to decreased retention of PGs [119], which is probably the result of early damage to the collagen network [108]. At the same time, alterations in PG aggregation are present in the early stages of AC degeneration [101,102]. Radin et al. [103] and Pelletier et al. [104] showed that repetitive loading of rabbit cartilage caused a loss of superficial PGs, which resulted in increased metabolic activity of chondrocytes, and thereby the formation of new PGs. This is supported by Lafeber et al. [119], Ryu et al. [120] and Teshima et al. [121], who found that synthesis and degradation of PGs are increased in OA cartilage.

4.3. Fibrillation

Fibrillation refers to the process in which the matrix becomes frayed and splits in the direction of the principal collagen fibrils [122,123]. Both the loss of PGs and loss of type II collagen are believed to cause superficial fibrillation [124,125].

4.4. Chondrocyte changes

In normal cartilage there is a delicate balance between synthesis and degradation. In OA, however, this balance is disturbed, with both degradation and synthesis usually enhanced [102,120]. Matrix degradation is caused by metalloproteinases, which cleave the matrix, and are secreted by cells both in the AC and the synovial tissue [126–129]. It has been shown that there is an increased proliferative activity in osteoarthritic chondrocytes [130,131]. This might be due to a better access to proliferative factors from the synovial fluid due to fissuring or loosening of the collagen network [130] or due to damage of the collagen network [132]. Several authors have suggested that cell death is a central feature in osteoarthritic cartilage degeneration [133–137]. Obviously dead cells can no longer maintain or repair the tissue. Moreover, because dead cells are not removed effectively from the cartilage, the products of cell death such as pyrophosphate and precipitated calcium may contribute to pathologic cartilage degradation.

5. Analytical and computational models of articular cartilage behavior

It is generally accepted that for a correct description of the mechanical behavior of AC at least a biphasic model should be used. According to the biphasic theory [68] the tissue is assumed to consist of an incompressible solid matrix, hydrated with an incompressible fluid. The total stress in the tissue is given by the sum of the solid and fluid stress [138],

$$\boldsymbol{\sigma}_{\mathrm{tot}} = \boldsymbol{\sigma}_{\mathrm{E}} - p\mathbf{I}, \tag{5.1}$$

where $\boldsymbol{\sigma}_{\mathrm{E}}$ is the effective stress tensor, p the hydrostatic fluid pressure, and $\mathbf{I}$ the unity tensor. In most biphasic models the solid matrix is assumed linear elastic and isotropic. For linear isotropic elasticity the effective stress tensor is given by

$$\boldsymbol{\sigma}_{\mathrm{E}} = \lambda e\mathbf{I} + 2\mu\boldsymbol{\varepsilon}, \tag{5.2}$$

where e is the dilatation, ε the strain tensor, and λ and μ are Lamé constants, which are functions of Young's modulus E and Poisson's ratio ν, as

$$\lambda = \frac{\nu E}{(1+\nu)(1-2\nu)}, \tag{5.3}$$

$$\mu = \frac{E}{2(1+\nu)}. \tag{5.4}$$

In the absence of mass exchange, the total mass change must be equal to the amount of fluid flow through the surface of the tissue. Hence, the law of conservation of mass is given by [138]

$$\nabla \cdot \vec{v}_{\mathrm{s}} + \nabla \cdot (n_{\mathrm{f}}(\vec{v}_{\mathrm{f}} - \vec{v}_{\mathrm{s}})) = 0, \tag{5.5}$$

where n_{f} is the fluid fraction, and $\vec{v}_{\mathrm{s}}$ and $\vec{v}_{\mathrm{f}}$ are the velocities of the solid and fluid phases, respectively. According to Darcy's law the fluid flux is related to the hydrostatic fluid pressure, as

$$n_{\mathrm{f}}(\vec{v}_{\mathrm{f}} - \vec{v}_{\mathrm{s}}) = -k\nabla p. \tag{5.6}$$

Here the left-hand term represents the fluid flow through the surface of the mixture and k is the hydraulic permeability. With Eq. (5.6) the law of conservation of mass, Eq. (5.5) becomes

$$\nabla \cdot \vec{v}_s + \nabla \cdot (k \nabla p) = 0. \tag{5.7}$$

As discussed in Section 2, the material properties of AC are depth-dependent. In several biphasic models this depth dependency has been included by using a depth-dependent aggregate modulus [139,140] or permeability [140].

The isotropic biphasic model has been used to analyze confined compression [141,142], unconfined compression [142,143], indentation [144–146], and impact [147,148] loading experiments, for normal and OA cartilage [149,150].

Although the linear biphasic model does include the fluid-flow-dependent viscoelasticity of AC, important features like strain-dependent permeability, anisotropy caused by the collagen network, flow-independent viscoelasticity and the swelling behavior of AC was not included. In Sections 5.1–5.4 extensions of the linear biphasic model, including these mechanisms are discussed.

5.1. Strain-dependent permeability

As discussed in Section 3, the permeability of cartilage is strain-dependent. According to Lai et al. [151] the strain-dependent permeability can be described by

$$k = k_0 \exp(M e_s), \tag{5.8}$$

where k_0 and M are material constants and e_s is the dilatation of solid matrix. In terms of the void ratio ($e = n_f/n_s$) this can be written as [152]:

$$k = k_0 \left(\frac{1+e}{1+e_0} \right)^M, \tag{5.9}$$

where and e and e_0 are the current and initial void ratios, respectively.

5.2. Anisotropy

Due to its complex collagen network, AC is highly anisotropic and has different properties in tension and compression. In the literature several models can be found that include these features. The most important or most widely used models are discussed in Sections 5.2.1–5.2.3.

5.2.1. Transversely isotropic models

In a transversely isotropic material it is assumed that all fibrils run in the same direction. Hence, a transversely isotropic material can be seen as an orthotropic material with one plane of isotropy. The direction parallel to the fibrils is called the longitudinal direction, and the directions perpendicular to the fibrils are called transversal directions. When assuming the fibrils to lie in the third direction, the stresses in the solid are given by [153]:

$$\begin{bmatrix} \sigma_{11} \\ \sigma_{22} \\ \sigma_{33} \\ \sigma_{12} \\ \sigma_{13} \\ \sigma_{23} \end{bmatrix} = \begin{bmatrix} \frac{1}{E_T} & -\frac{\nu_{TT}}{E_T} & -\frac{\nu_{LT}}{E_L} & 0 & 0 & 0 \\ -\frac{\nu_{TT}}{E_T} & \frac{1}{E_T} & -\frac{\nu_{LT}}{E_L} & 0 & 0 & 0 \\ -\frac{\nu_{TL}}{E_T} & -\frac{\nu_{TL}}{E_T} & \frac{1}{E_L} & 0 & 0 & 0 \\ 0 & 0 & 0 & \frac{1}{G_L} & 0 & 0 \\ 0 & 0 & 0 & 0 & \frac{1}{G_L} & 0 \\ 0 & 0 & 0 & 0 & 0 & \frac{1}{G_T} \end{bmatrix}^{-1} \begin{bmatrix} \varepsilon_{11} \\ \varepsilon_{22} \\ \varepsilon_{33} \\ \gamma_{12} \\ \gamma_{13} \\ \gamma_{23} \end{bmatrix}, \tag{5.10}$$

where E_L and E_T are the longitudinal and transversal Young's moduli, respectively, G_L is the longitudinal shear modulus, and V_{LT}, V_{TT} and V_{TL} the Poisson's ratios that give the strain in either longitudinal (along the fibrils) or transversal (perpendicular to the fibrils) direction for a stretch in the other direction. The transversal shear modulus G_T is given by

$$G_T = \frac{E_T}{2(1+\nu_{TT})}. \tag{5.11}$$

Because of symmetry

$$\frac{\nu_{LT}}{E_L} = \frac{\nu_{TL}}{E_T}. \tag{5.12}$$

This leaves five independent material parameters (E_L, E_T, ν_{LT}, ν_{TT} and G_L). In several studies such transversely isotropic biphasic models were used [142,148,154].

5.2.2. Conewise linear elastic model

In the isotropic and transversely isotropic models the material has the same properties in compression and tension. Isotropic conewise elasticity models take the compression–tension nonlinearity of the tissue into account [155], while

still being linear. In this model the solid stress is given by

$$\boldsymbol{\sigma}_{\mathrm{E}} = \sum_{a=1}^{3} \left(\lambda_1(\mathbf{A}_a : \boldsymbol{\varepsilon}) \operatorname{tr}(\mathbf{A}_a \boldsymbol{\varepsilon}) \mathbf{A}_a + \sum_{b=1, b\neq a}^{3} \lambda_2 \operatorname{tr}(\mathbf{A}_a \boldsymbol{\varepsilon}) A_b \right) + 2\mu\boldsymbol{\varepsilon}, \tag{5.13}$$

where $\boldsymbol{\varepsilon}$ is the elastic strain tensor and $\mathbf{A}_a$ is a tensor corresponding to three material directions, defined by unit vectors $\mathbf{a}_a$. Compression–tension nonlinearity occurs when the Lamé constant λ_1 is dependent on the normal strain along direction $\mathbf{a}_a$:

$$\lambda_1(\mathbf{A}_a : \boldsymbol{\varepsilon}) = \begin{cases} \lambda_{-1}, & \mathbf{A}_a : \boldsymbol{\varepsilon} < 0, \\ \lambda_{+1}, & \mathbf{A}_a : \boldsymbol{\varepsilon} > 0. \end{cases} \tag{5.14}$$

The aggregate modulus in compression and tension is then given by $H_{-\mathrm{A}} = \lambda_{-1} + 2\mu$ and $H_{+\mathrm{A}} = \lambda_{+1} + 2\mu$, respectively. λ_2 is the "off-diagonal" modulus, determined from confined compression as a ratio of radial stress to axial strain at equilibrium [156].

In summary, the conewise linear elasticity model has five material parameters: aggregate modulus in compression and tension, $H_{-\mathrm{A}}$ and $H_{+\mathrm{A}}$, respectively, "off-diagonal" modulus λ_2, shear moduli μ and permeability k. Both confined and unconfined compression, torsional shear tests and tensile tests for cartilage were analyzed with this model [79,155,157].

5.2.3. Fibril-reinforced models

Another way to include the compression–tension nonlinearity of the solid matrix is by using a fibril-reinforced model. In a fibril-reinforced model [158–166] the fibril network (collagen network) contributes to the mechanical stiffness of the material, in addition to the isotropic matrix. The solid stress of a fibril-reinforced material is given by the sum of the matrix and fibril stresses. In the literature two kinds of fibril-reinforced models can be found, spring models and continuum models. In spring models, fibrils are represented by springs between the nodes of the elements. Hence, the fibrils can only be represented in the direction of the elements. The solid stress of a fibril-reinforced material is given by the sum of the matrix and fibril stresses [158], as

$$\boldsymbol{\sigma}_{\mathrm{E},i} = \sigma_{\mathrm{m},i} + \sigma_{\mathrm{f},i}, \tag{5.15}$$

where $\sigma_{\mathrm{m},i}$ and $\sigma_{\mathrm{f},i}$ represent the normal stresses in direction i, in the nonfibrillar matrix and the collagen fibrils, respectively. The most sophisticated spring-based fibril-reinforced models are those of Li et al. [159–164]. In their earlier models the stiffness of the collagen fibrils was represented by a linear spring with stiffness E_0, parallel to a nonlinear spring with stiffness $E_1 = E_\varepsilon \varepsilon_{\mathrm{f}}$ (Fig. 4a), where ε_{f} is the strain in the fibril direction. The fibril stress σ_{f} in these models was then given by

$$\sigma_{\mathrm{f}} = \begin{cases} (E_0 + E_\varepsilon \varepsilon_{\mathrm{f}})\varepsilon_{\mathrm{f}} & \text{for } \varepsilon_{\mathrm{f}} \geq 0, \\ 0 & \text{for } \varepsilon_{\mathrm{f}} < 0. \end{cases} \tag{5.16}$$

In their most recent model [164] the fibrils were assumed viscoelastic and the fibril stresses were given by

$$\sigma_{\mathrm{f}} = \sigma_0(0) + \int_0^t G(t-\tau) E_{\mathrm{f}}(\varepsilon_{\mathrm{f}}) \dot{\varepsilon}_{\mathrm{f}} \, \mathrm{d}\tau, \tag{5.17}$$

where the relaxation function is represented by a spectrum approximation as

$$G(t) = 1 + \sum_{M} g_{\mathrm{m}} \exp\left(-\frac{t}{\lambda_{\mathrm{m}}}\right) \tag{5.18}$$

with λ_{m} the characteristic times for viscoelastic dissipation.

In the continuum fibril-reinforced models [165,166] the fibril orientation is independent of the mesh. Hence, the fibrils can run in any direction, which enables the representation of a geometrically realistic collagen network. In these models the solid stress is given by

$$\boldsymbol{\sigma}_{\mathrm{E}} = \sigma_{\mathrm{m}} + \sum_{i=1}^{\mathrm{tot}\, f} \sigma_{\mathrm{f},i} \cdot \vec{v}_{\mathrm{new},i} \otimes \vec{v}_{\mathrm{new},i}, \tag{5.19}$$

where $\sigma_{\mathrm{f},i}$ are fibril stresses in the ith fibril and $\vec{v}_{\mathrm{new},i}$ the current fibril direction of the ith fibril.

In the models of Wilson et al. [165,166,189] the collagen fibrils were assumed to be viscoelastic and were represented by a linear spring with stiffness E_0, parallel to a nonlinear spring with stiffness $E_1 = E_\varepsilon \varepsilon_{\mathrm{f}}$ in series with a linear dashpot with damping constant η (Fig. 4b). Assuming that the fibrils only resist tension, the stresses in the viscoelastic fibrils are

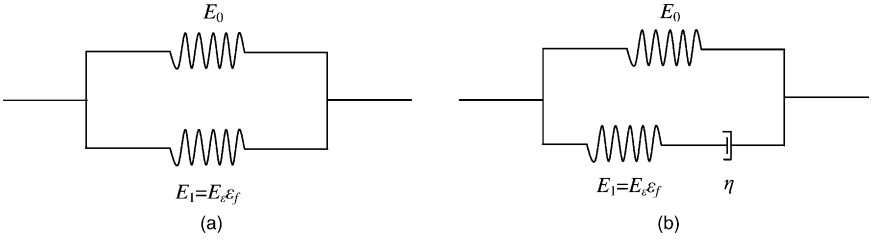

Fig. 4. Schematic models for elastic collagen fibrils (a) and viscoelastic collagen fibrils (b).

given by

$$\sigma_f = -\frac{\eta}{2\sqrt{(\sigma_f - E_0\varepsilon_f)E_\varepsilon}}\dot{\sigma}_f + E_0\varepsilon_f + \left(\eta + \frac{\eta E_0}{2\sqrt{(\sigma_f - E_0\varepsilon_f)E_\varepsilon}}\right)\dot{\varepsilon}_f \quad \text{for} \quad \varepsilon_f > 0$$
$$\sigma_f = 0 \qquad\qquad\qquad\qquad\qquad\qquad\qquad\qquad\qquad\qquad\qquad\qquad \text{for} \quad \varepsilon_f \leq 0 \tag{5.20}$$

The most significant differences between the spring-based fibril-reinforced and the transversely isotropic model is that the fibrils in the fibril-reinforced model resist only tension, while the transversely isotropic model has the same stiffness in compression and tension. The main difference with the conewise linear elastic model is that nonlinear properties of the fibrils can be included. An additional advantage of the continuum fibril-reinforced models is that the fibrils can run in any direction.

The spring-based fibril-reinforced biphasic models [158–164] have been applied in unconfined compression, mainly for the characterization of the role of the collagen network in cartilage time-dependent response. Korhonen et al. [167] used this model to study the roles of proteoglycan depletion and collagen degeneration on the mechanical behavior of AC.

The continuum fibril-reinforced poroviscoelastic model was successfully used to describe confined compression, unconfined compression and indentation [165,166].

5.3. Flow-independent viscoelasticity (poroviscoelastic models)

As discussed in Section 3 the time-dependent behavior of AC is caused by both fluid-flow-dependent and flow-independent viscoelasticity. In a poroviscoelastic model both types are included. Two different poroviscoelastic models can be found in the literature. In the first, the solid matrix is only viscoelastic in shear [168] and in the second the solid matrix is viscoelastic both in shear and bulk deformation [57]. The solid stress of these models is given by

$$\boldsymbol{\sigma}_{\mathrm{E}} = \lambda e\mathbf{I} + 2\mu\int_0^t G(t-\tau)\frac{\partial \mathbf{e}}{\partial \tau}\,\mathrm{d}\tau, \tag{5.21}$$

and

$$\boldsymbol{\sigma}_{\mathrm{E}} = \lambda\int_0^t G(t-\tau)\frac{\partial e\mathbf{I}}{\partial \tau}\,\mathrm{d}\tau + 2\mu\int_0^t G(t-\tau)\frac{\partial \mathbf{e}}{\partial \tau}\,\mathrm{d}\tau, \tag{5.22}$$

respectively. Here τ is a relaxation time constant and $\mathbf{e}$ the deviatoric component of the elastic strain tensor. The relaxation function $G(t)$ is given by [168]

$$G(t) = 1 + \int_0^\infty S(\tau)\,\mathrm{e}^{-t/\tau}, \tag{5.23}$$

where the continuous relaxation spectrum $S(\tau)$ is given by

$$S(\tau) = \begin{cases} \dfrac{c}{\tau} & \text{for } \tau_1 \leq \tau \leq \tau_2, \\ 0 & \text{for } \tau < \tau_1, \tau > \tau_2, \end{cases} \tag{5.24}$$

where τ_1 and τ_2 are the short and long-term relaxation time constants, respectively, and c is the magnitude of the relaxation power spectrum.

In addition to the biphasic material parameters in the isotropic case, the poroviscoelastic model adds three more parameters, which are a discrete spectrum value c, a short-term relaxation time constant τ_1 and a long-term relaxation time constant τ_2.

The poroviscoelastic model was applied for the characterization of time-dependent response of normal [73,168–171] and degenerated [73,171] cartilage in confined compression, unconfined compression and indentation.

Other models that also include both fluid-flow-dependent and flow-independent viscoelasticity are the fibril-reinforced ones of Li et al. [164] and Wilson et al. [165,166]. The main difference between these models and the regular poroviscoelastic ones is that in these the viscoelastic behavior of the solid is solely ascribed to the collagen network. Hence, the viscoelastic nature of the solid is highly dependent on the orientation of the collagen fibrils. Another important difference is that in the fibril-reinforced models the solid is viscoelastic in tension, while regular poroviscoelastic models are viscoelastic for both compression and tension. But the main difference between the models is that the fibril-reinforced ones included the anisotropy of the solid matrix.

5.4. Swelling

As discussed in Section 3 there are two mechanisms that cause swelling of cartilage: (1) osmotic swelling, which is due to an excess in ion particles inside the tissue, and (2) chemical expansion, which is caused by repulsion of the closely spaced negatively charged groups of the PGs. The next two paragraphs discuss how these mechanisms were included in numerical models.

5.4.1. Osmotic swelling

5.4.1.1. Mechano-electrochemical model. In the last decade several mechano-electrochemical models were developed that include the influence of ion concentration and ion fluxes, and therefore enable a representation of AC swelling behavior. Lai et al. [77] derived a small deformation mechano-electrochemical extension of the biphasic model that included three phases: an incompressible solid, an incompressible fluid and a monovalent ionic phase. This theory was generalized to finite deformations by Huyghe and Janssen [138]. These mechano-electrochemical models are also known as triphasic or quadriphasic ones. Below, a short summary of the most

important equations of the mechano-electrochemical theory are given.

The total stress is the same as for the biphasic model (Eq. (5.1)), but in this case the hydrostatic pressure is given by [138]

$$p = \mu^{\mathrm{f}} + \Delta\pi, \tag{5.25}$$

where μ^{f} is the electrochemical potential and $\Delta\pi$ the osmotic pressure gradient.

In the absence of mass exchange the law of conservation of mass is given by [138]:

$$\frac{\partial}{\partial t} n_\alpha + \nabla \cdot (n_\alpha(v_\alpha - v_{\mathrm{s}})) = 0, \tag{5.26}$$

where n_α and v_α are volume fraction and velocity of component α, respectively. The relation between permeability and ion diffusion–convection, and the velocity of component α, are described by [172]:

$$-c_\beta \nabla \mu^\beta = \sum_{\alpha=f,+,-} \mathbf{B}_{\beta\alpha}(v_\alpha - v_{\mathrm{s}}), \quad \beta = f, +, -, \tag{5.27}$$

where c_β is the molecular concentration of phase β per unit of mixture volume, μ^β its molecular potential and $\mathbf{B}_{\beta\alpha}$ a symmetric matrix of frictional coefficients.

The osmotic pressure gradient from Eq. (5.25) is given by

$$\Delta\pi = \pi - \pi_{\mathrm{ext}}, \tag{5.28}$$

where internal and external osmotic pressures are given as [138]:

$$\pi = \phi_{\mathrm{int}} RT(c^+ + c^-) \tag{5.29}$$

and

$$\pi_{\mathrm{ext}} = \phi_{\mathrm{ext}} RT(c^+_{\mathrm{ext}} + c^-_{\mathrm{ext}}),$$

respectively. Here R is the gas constant, T the absolute temperature, c^+ and c^- are the concentrations of mobile cations (Na^+) and anions (Cl^-) (M), respectively, ϕ_{ext} are the internal and external osmotic coefficients, respectively. At each point in the tissue electroneutrality must hold, hence

$$c^+ = c^- + c_{\mathrm{F}}, \tag{5.30}$$

where c_{F} is the FCD. The chemical potential per mole of NaCl in the external solution μ_{ext} and that in the tissue μ are given by [77]:

$$\begin{aligned}\mu_{\mathrm{ext}} &= \mu_{0,\mathrm{ext}} + RT\ln(\gamma^+_{\mathrm{ext}} c^+_{\mathrm{ext}}) + RT\ln(\gamma^-_{\mathrm{ext}} c^-_{\mathrm{ext}}) \\ &= \mu_{0,\mathrm{ext}} + RT\ln(\gamma^{\pm 2}_{\mathrm{ext}} c^2_{\mathrm{ext}}),\end{aligned} \tag{5.31}$$

$$\begin{aligned}\mu &= \mu_0 + RT\ln(\gamma^+_{\mathrm{int}} c^+) + RT\ln(\gamma^-_{\mathrm{int}} c^-) \\ &= \mu_0 + RT\ln((\gamma^{\pm}_{\mathrm{int}})^2 c^-(c^- + c_{\mathrm{F}})),\end{aligned} \tag{5.32}$$

where $\gamma^{\pm}_{\mathrm{int}}$ and $\gamma^{\pm}_{\mathrm{ext}}$ are the mean activity coefficients and μ_0 the concentration-independent potential.

The internal equilibrium ion concentrations are given by [138]:

$$c^{\pm} = \frac{\pm c_{\mathrm{F}} + \sqrt{c^2_{\mathrm{F}} + 4\frac{(\gamma^{\pm}_{\mathrm{ext}})^2}{(\gamma^{\pm}_{\mathrm{int}})^2} c^2_{\mathrm{ext}}}}{2}. \tag{5.33}$$

The internal osmotic pressures in equilibrium can then be given by

$$\pi = \phi_{\mathrm{int}} RT(c^+ + c^-) = \phi_{\mathrm{int}} RT \sqrt{c^2_{\mathrm{F}} + 4\frac{(\gamma^{\pm}_{\mathrm{ext}})^2}{(\gamma^{\pm}_{\mathrm{int}})^2} c^2_{\mathrm{ext}}}. \tag{5.34}$$

Mechano-electrochemical models were used to describe the swelling behavior of articular cartilage [77] and intervertebral discs in 1D [173,174] and 3D [175].

5.4.1.2. Biphasic swelling model. Based on the hypothesis that electrolyte flux can be neglected in mechanical and diffusion studies of charged materials [176], Wilson et al. [177] have recently developed a biphasic swelling model. For this model, which is a simplification of the full mechano-electrochemical model [77,173], it was assumed that the ion concentration is always in equilibrium. Just as in the full mechano-electrochemical model the solid stress is given by

$$\boldsymbol{\sigma} = -(\mu^{\mathrm{f}} + \Delta\pi)\mathbf{I} + \boldsymbol{\sigma}_{\mathrm{s}}, \tag{5.35}$$

Since the osmotic components are assumed to equilibrate instantaneously with the external bath, only the ion concentrations in equilibrium must be determined. Hence, the ion concentrations are always given by Eq. (5.33), so that the osmotic pressure gradient in equilibrium is given by

$$\Delta\pi = \phi_{\mathrm{int}} RT \sqrt{c^2_{\mathrm{F}} + 4\frac{(\gamma^{\pm}_{\mathrm{ext}})^2}{(\gamma^{\pm}_{\mathrm{int}})^2} c^2_{\mathrm{ext}}} - 2\phi_{\mathrm{ext}} RT c_{\mathrm{ext}}. \tag{5.36}$$

When assuming that the external salt concentration and temperature remain constant, the only nonconstant in this equation is FCD (c_{F}), which can be expressed as a function of the tissue deformation, as

$$c_{\mathrm{F}} = c_{\mathrm{F},0}\left(\frac{n_{\mathrm{f},0}}{n_{\mathrm{f},0} - 1 + J}\right), \tag{5.37}$$

where $n_{\mathrm{f},0}$ is the initial fluid fraction, $c_{\mathrm{F},0}$ the initial FCD and J the determinant of the deformation tensor $\mathbf{F}$. Since the osmotic pressure in equilibrium is only a function of the deformation tensor $\mathbf{F}$, it can easily be implemented in commercial FEA packages.

It has recently shown that, depending on the material properties, the overall deformational behavior of the full mechano-electrochemical and biphasic swelling models are similar [177]. Hence, the biphasic swelling model can be a good alternative for the complex mechano-electrochemical model. Since the ion flux in the biphasic swelling model is assumed

infinitely fast, this model can obviously not be used to investigate ion fluxes in soft hydrated tissues.

5.4.2. Chemical expansion

The dependence of the chemical expansion stress T_c on the ion concentration was not quantified based on a strict theory. Eisenberg and Grodzinsky [178] proposed for the chemical expansion stress

$$T_c = \beta_0 \exp\left(\frac{c}{c_\beta}\right) \tag{5.38}$$

with β_0 and c_β the material constants, and c the effective NaCl concentration, which is a function of c^+ and c^-, as

$$c = c^{\pm}\sqrt{1 \pm \frac{c_F}{c^{\pm}}}. \tag{5.39}$$

Another form of T_c was proposed by Lai et al. [77], as

$$T_c = a_0 c_F \exp\left(-\kappa \frac{\gamma^{\pm}_{ext}}{\gamma^{\pm}_{int}}\sqrt{c^-(c^- + c_F)}\right), \tag{5.40}$$

with a_0 and κ material constants.

The chemical expansion stress can be included in both the full mechano-electrochemical and the biphasic swelling models. When it is included in a full mechano-electrochemical model, c^- follows from Eqs. (5.26) and (5.27). When it is implemented in a biphasic swelling model, c^- is given by Eq. (5.33). Hence, in a biphasic swelling model the chemical expansion stress is also only a function of the FCD and thereby the deformation of the tissue.

6. Recapitulation

6.1. Analysis of the mechanical behavior of AC

It was shown that the linear biphasic model can account for creep and stress relaxation during confined compression [68,72]. Also the long-term creep response can be accounted for, but significant deviations are seen for the short-term response of the tissue [57,145]. Furthermore, the utility of this model diminishes when the tissue is subjected to unconfined compression [143,179,180]. The main reason for this is probably that the anisotropy, which plays an important role during this test, is not included in this type of model.

DiSilvestro et al. [169] showed that in unconfined compression the transversely isotropic biphasic model was able to account for either the measured lateral displacement or the measured reaction force very well, but could not account for both variables simultaneously. To be able to describe the lateral displacement, a very small value for the Young's modulus is needed (9.74 Pa) [142,169]. This is probably caused by the absence of flow-independent viscoelasticity, due to which the lateral stiffness remains too high. Hence, transverse anisotropy still cannot fully account for the behavior of AC during unconfined compression.

Neither can the isotropic conewise elasticity model account for lateral displacements and reaction forces simultaneously, due to the absence of flow-independent viscoelasticity. However, Soltz and Ateshian [155] showed that it can account for the reaction force during confined and unconfined compression, and the fluid pressure at the center of the sample during unconfined compression, simultaneously.

The linear poroviscoelastic model, which does include flow-independent viscoelasticity, is able to simultaneously account for reaction forces and lateral displacements during unconfined compression [169]. Moreover, the poroviscoelastic model is able to simultaneously account for experimental data measured from unconfined compression and either indentation or confined compression [168]. It was also reported that the poroviscoelastic model can accurately simulate unconfined compression at varying strain rates [170]. Although this model includes fluid-independent viscoelasticity, it lacks the anisotropy and compression–tension nonlinearity of the tissue, which is probably the reason why not all these tests can be accounted for simultaneously.

Huang et al. [79] therefore combined the conewise elasticity and the poroviscoelastic models. They demonstrated that this combination, which includes both flow-independent viscoelastic and tension–compression nonlinearity of the solid matrix, can simultaneously account for the response of AC during unconfined compression at different loading rates and its response to dynamic loading. They showed that their model produced better predictions of the dynamic modulus of cartilage in unconfined dynamic compression than the biphasic conewise-linear elasticity and poroviscoelastic models, indicating that intrinsic viscoelasticity and tension–compression nonlinearity of AC both play important roles in the load–support mechanism of cartilage. The only other models that also include these two features are the fibril-reinforced poroviscoelastic models of Li et al. [164] and Wilson et al. [165,166].

According to Li et al. [159] the influence of strain-dependent fibril stiffness on the nonlinear mechanical behavior is much larger than the effect of strain-dependent permeability. The only models that include the effect of a strain-dependent fibril stiffness are the fibril-reinforced models of Li et al. [159–164] and Wilson et al. [165,166]. As mentioned above, three of these also include the viscoelastic behavior of the collagen fibrils [164–166]. It was recently shown that fibrils at the same location can be stressed differently, depending on the architecture of the collagen network [165]. Hence, it is important that the collagen network is described as realistic as possible. In the spring-based fibril-reinforced models the fibril directions are coupled to the element shapes. Hence, although these models can be used to include the anisotropic nature of the collagen network, collagen structures as seen in AC cannot be included. The only model that does account for this is the continuum based fibril-reinforced poroviscoelastic model of Wilson et al. [165,166]. This model is also the only model that showed the ability to simultaneously account for the reaction force in confined

compression, unconfined compression and indentation, and the lateral deformation during unconfined compression.

If one also wants to include the swelling behavior, the models as mentioned above can be combined with the full mechano-electrochemical [75,77,138,173,174] or biphasic swelling model [176,177]. It was recently shown that depending on the material properties the deformation behavior of these models is similar [177]. The difference between them is that the full mechano-electrochemical description can account for ion fluxes, while the biphasic one is computationally less expensive and that it is also applicable for large deformations.

The only models in which swelling is combined with the collagen structure of the tissue are those of Sun and Leong [175] and Wilson et al. [166]. The latter have shown that they can simultaneously account for reaction force during ID swelling, confined compression, indentation and unconfined compression, as well as the lateral deformation during unconfined compression [166]. Although the model of Sun and Leong [175] was originally made to study the intervertebral disc, we believe that it is also suitable for AC. The main difference between the models is that the model of Wilson et al. [166] can account for large deformations, and that it includes the viscoelastic behavior of the collagen fibrils, while the model of Sun and Leong [175] can account for transport inside the tissue.

6.2. Damage analysis

The only cartilage damage analyses in the literature using FEA modeling are simulations of impact loading. In these studies the locations of cracks were compared to locations of maximal stresses and strains, as computed using both linear elastic and biphasic formulations. It was suggested that cracks at the articular surface could be explained using a maximal shear stress [181], a tensile stress [182], or a maximal principal strain criterion [80,183,184]. Cracks along the tidemark could be explained by excessive shear stresses at the cartilage–bone interface [92,183–185]. With FEA models of cylindrical cartilage plug, Garcia et al. [148] computed the distribution of maximal shear stresses in the AC during impact loading, using both an isotropic and a transversely isotropic description of cartilage properties. They found that with an isotropic material description, cracks along the tidemark can be explained, and that with a transversely isotropic material description cracks at the articular surface can be explained; neither of these models could explain both types of damage. The same results were found for cartilage damage after meniscectomy [186]. None of these studies considered the mechanics of the microstructure of AC, nor did they study the changes in cartilage before formations of the cracks.

Of the models discussed in the previous section, several models were used to analyze the mechanical behavior of degenerated cartilage [73,149,150,167,171]. However, the initiation and progression of cartilage degeneration has so far not been studied.

As previously indicated, collagen damage and subsequent swelling are thought to be the initial signs of AC damage. Models which include descriptions of the collagen network have only recently become available. These models are thought to significantly accelerate progression in this field of research in the next decade. Also the biphasic swelling model is an interesting alternative for the better known full mechano-electrochemical model, as simulations of larger geometries (i.e. whole joints rather than small cartilage samples) come within reach. Another important recent development is the introduction of multilevel FEA method [187], enabling evaluation of the microstructural influences on the macroscopic stresses and strains, and vice versa.

7. Conclusion

It can be concluded that the requirements of a material model are highly dependent on the research question. In general, the more features of the composition and structure of AC are included, the larger the number of material parameters that must be determined, and the more computationally expensive the model becomes. Hence, one should always try to use the simplest model that is sufficient to obtain the required data. The present overview can assist in selecting that.

As FEA analysis enables calculations of stresses and strains in the different components of AC, it can be a useful tool to study the onset and development of mechanically induced cartilage damage, as well as for understanding the mechanical behavior of healthy and degenerated cartilage. We believe that FEA modeling will help us to understand normal cartilage functioning, the degeneration process of AC, and eventually provide tools for developing preventive measures and treatments for diseases like osteoarthritis.

References

[1] Mow VC, Ateshian GA. Lubrication and wear of diarthrodial joints. In: Mow VC, Hayes WC, editors. Basic orthopaedic biomechanics. 2nd ed. Philadelphia: Lippincott-Raven; 1997. p. 275–315.
[2] Mow VC, Ateshian GA, Spilker RL. Biomechanics of diarthrodial joints: a review of twenty years of progress. J Biomech Eng 1993;115:460–7.
[3] Radin EL, Burr DB, Fyhrie D, Brown TD, Boyd RD. Characteristics of joint loading as it applies to osteoarthrosis. In: Biomechanics of diarthrodial joints I. New York: Springer-Verlag; 1990.
[4] Maroudas A. Biophysical chemistry of cartilaginous tissues with special reference to solute and fluid transport. Biorheology 1975;12:233–48.
[5] Buckwalter JA, Hunziker EB, Rosenberg LC, Coutts R, Adams M, Eyre D. Articular cartilage: composition and structure. In: Wo SI, Buckwalter JA, editors. Injury and repair of musculoskeletal soft tissues. 2nd ed. Park Ridge: American Academy of Orthopaedic Surgeons; 1991. p. 405–25.
[6] Heinegard D, Oldberg A. Structure and biology of cartilage and bone matrix noncollagenous macromolecules. FASEB J 1989;3(9): 2042–51.

[7] Maroudas A. Physicochemical properties of articular cartilage. In: Freeman MAR, editor. Adult articular cartilage. 2nd ed. Kent, UK: Pitman Med.; 1979. p. 215–323.
[8] Urban JPG, Maroudas A, Bayliss MT, Dillon J. Swelling pressures of PG's at the concentrations found in cartilagenous tissues. Biorheology 1979;16:447–64.
[9] Mow VC, Guo XE. Mechano-electrochemical properties of articular cartilage: their inhomogeneities and anisotropies. Annu Rev Biomed Eng 2002;4:175–209.
[10] Cremer MA, Rosloniec EF, Kang AH. The cartilage collagens: a review of their structure, organization, and role in the pathogenesis of experimental arthritis in animals and in human rheumatic disease. J Mol Med 1998;76:275–88.
[11] Hasler EM, Herzog W, Wu JZ, Muller W, Wyss U. Articular cartilage biomechanics: theoretical models, material properties, and biosynthesis response. Clin Rev Biomech Eng 1999;27:415–88.
[12] Eyre DR. The collagens of articular cartilage. Sem Arthritis Rheum 1991;21:2–11.
[13] Clark JM. Variation of collagen fiber alignment in a joint surface: a scanning electron microscope study of the tibial plateau in dog, rabbit, and man. J Orthop Res 1991;9:246–57.
[14] Clarke IC. Articular cartilage: a review and scanning electron microscope study. 1. The interterritorial fibrillar architecture. J Bone Joint Surg Br 1971;53:732–50.
[15] Benninghoff A. Form und bau der gelenkknorpel in ihren beziehungen zur funktion. Z Zellforsch 1925;2:783–862.
[16] Akizuki S, Mow VC, Muller F, Pita JC, Howell DS, Manicourt DH. Tensile properties of human knee joint cartilage. I. Influence of ionic conditions, weight bearing, and fibrillation on the tensile modulus. J Orthop Res 1986;4(4):379–92.
[17] Kempson GE, Freeman MA, Swanson SA. Tensile properties of articular cartilage. Nature 1968;220(172):1127–38.
[18] Roth V, Mow VC. The intrinsic tensile behavior of the matrix of bovine articular cartilage and its variation with age. J Bone Joint Surg Am 1980;62:1102–17.
[19] Woo SY, Akeson WH, Jemmott GF. Measurements of nonhomogeneous directional mechanical properties of articular cartilage in tension. J Biomech 1976;9:785–91.
[20] Mow VC, Zhu W, Ratclife A. Structure and function of articular cartilage and meniscus. In: Mow VC, Hayes WC, editors. Basic orthopaedic biomechanics. New York: Raven Press; 1991. p. 143–98.
[21] Silyn-Roberts H, Broom ND. Fracture behaviour of cartilage-on-bone in response to repeated impact loading. Connect Tiss Res 1990;24:143–56.
[22] Broom N, Chen MG, Hardy A. A degeneration-based hypothesis for interpreting fibrillar changes in the osteoarthritic cartilage matrix. J Anat 2001;199(Pt 6):683–98.
[23] Broom ND, Marra DL. Ultrastructural evidence for fibril-to-fibril associations in articular cartilage and their functional implication. J Anat 1986;146:185–200.
[24] Broom ND, Silyn-Roberts H. The three-dimensional 'knit' of collagen fibrils in articular cartilage. Connect Tiss Res 1989;23(4): 261–77.
[25] Chen MH, Broom N. On the ultrastructure of softened cartilage: a possible model for structural transformation. J Anat 1998;192:329–41.
[26] Eyre DR, Apones S, Wu JJ, Ericksson LH, Walsh KA. Collagen type IX: evidence for covalent linkages to type II collagen in cartilage. FEBS Lett 1987;220:337–41.
[27] Wu JJ, Woods PE, Eyre DR. Identification of cross-linking sites in bovine cartilage type IX collagen reveals an antiparallel type II–type IX molecular relationship and type IX to type IX bonding. J Biol Chem 1992;267:23007–14.
[28] Yasui K. Three-dimensional architecture of human normal menisci. J Jpn Orthop Assoc 1978;52:391–9.
[29] Kempson GE, Tuke MA, Dingle JT, Barrett AJ, Horsfield PH. The effects of proteolytic enzymes on the mechanical properties of adult human articular cartilage. Biochim Biophys Acta 1976;428:741–60.
[30] Maroudas A. Balance between swelling pressure and collagen tension in normal and degenerate cartilage. Nature 1976;260:808–9.
[31] Mow VC, Ratcliffe A, Poole AR. Cartilage and diarthrodial joints as paradigms for hierarchical materials and structures. Biomaterials 1992;13:67–97.
[32] Schmidt MB, Chun LE, Eyre DR, Mow VC. The relationship between collagen cross-linking and tensile properties of articular cartilage. Trans ORS 1987;12:134.
[33] Ghivizzani SC, Oligino TJ, Robbins PD, Evans CH. Cartilage injury and repair. Phys Med Rehabil Clin N Am 2000;11(2):289–307.
[34] Junqueira LC, Carneiro J. Basic histology. 4th ed. Los Altos: Lange Medical; 1983. p. 129.
[35] Verzijl N, DeGroot J, Ben ZC, Brau-Benjamin O, Maroudas A, Bank RA, et al. Cross-linking by advanced glycation end products increases the stiffness of the collagen network in human articular cartilage: a possible mechanism through which age is a risk factor for osteoarthritis. Arthritis Rheum 2002;46(1):114–23.
[36] Bank RA, Bayliss MT, Lafeber FP, Maroudas A, TeKoppele JM. Ageing and zonal variation in post-translational modification of collagen in normal human articular cartilage. The age-related increase in non-enzymatic glycation affects biomechanical properties of cartilage. Biochem J 1998;330(Pt 1):345–51.
[37] Chen AC, Temple MM, Ng DM, Richardson CD, DeGroot J, Verzijl N. Age related cross-linking alters tensile properties of articular cartilage. Trans Orthop Res Soc 2001;26:128.
[38] Takahashi M, Kushida K, Ohishi T, Kawana K, Hoshino H, Uchiyama A, et al. Quantitative analysis of cross-links pyridinoline and pentosidine in articular cartilage of patients with bone and joint disorders. Arthritis Rheum 1994;37(5):724–8.
[39] Uchiyama A, Ohishi T, Takahashi M, Kushida K, Inoue T, Fujie M, et al. Fluorophores from aging human articular cartilage. J Biochem (Tokyo) 1991;110(5):714–8.
[40] Verzijl N, DeGroot J, Oldehinkel E, Bank RA, Thorpe SR, Baynes JW, et al. Age-related accumulation of Maillard reaction products in human articular cartilage collagen. Biochem J Sep 2000;350(Pt 2):381–7.
[41] Stockwell RA. Biology of cartilage cells. Cambridge: Cambridge University Press; 1979.
[42] Urban JP, Holm S, Maroudas A, Nachemson A. Nutrition of the intervertebral disc: effect of fluid flow on solute transport. Clin Orthop 1982;170:296–302.
[43] Urban JP. The chondrocyte: a cell under pressure. Br J Rheum 1994;33:908–10.
[44] Grodzinsky AJ, Frank EH, Kim YJ, Buschmann MD. The role of specific macromolecules in cell-matrix interactions and in matrix function: physiochemical and mechanical mediators of chondrocyte biosynthesis. In: Comper WD, editor. Extracellular matrix, vol. II: molecular components and interactions. Amsterdam: Harwood Academic Publishers; 1996. p. 310–34.
[45] Muir H, Bullough P, Maroudas A. The distribution of collagen in human articular artilage with some of its physical implications. J Bone Joint Surg 1970;52:554–63.
[46] Wong M, Wuethrich P, Eggli P, Hunziker EB. Zone-specific cell biosynthesis activity in mature bovine articular cartilage: a new method using confocal microscopic stereology and quantitative autoradiography. J Orthop Res 1996;14:424–32.
[47] Hunziker E. Articular artilage structure in humans and experimental animals. In: Kuettner KE, Peyron JG, Schleyer R, Hascall VC, editors. Articular cartilage and osteoarthritism. New York: Raven Press; 1992. p. 183–99.
[48] Hunziker EB, Michel M, Studer D. Ultrastructure of adult human cartilage matrix after cryotechnical processing. Microsc Res Technol 1997;37:271–84.

[49] Torzilli PA, Arduino JM, Gregory JD, Bansal M. Effect of proteoglycan removal on solute mobility in articular cartilage. J Biomech 1997;30:895–902.
[50] Wong M, Wuethrich P, Buschmann MD, Eggli P, Hunziker EB. Chondrocyte biosynthesis correlates with local tissue strain in statically compressed adult articular cartilage. J Orthop Res 1997;15:189–96.
[51] Bullough PG, Jagannath A. The morphology of the calcification front in articular cartilage. Its significance in joint function. Bone Joint Surg Br 1983;65:72–8.
[52] Oegema Jr TR, Carpenter RJ, Hofmeister F, Thompson Jr RC. The interaction of the zone of calcified cartilage and subchondral bone in osteoarthritis. Microsc Res Technol 1997;37:324–32.
[53] Mente PL, Lewis JL. Elastic modulus of calcified cartilage is an order of magnitude less than that of subchondral bone. J Orthop Res 1994;12:637–47.
[54] Mow VC, Lai WM, Eisenfeld J, Redler I. Some surface characteristics of articular cartilage. II. On the stability of articular surface and a possible biomechanical factor in etiology of chondrodegeneration. J Biomech 1974;7:457–68.
[55] Mak AF. The apparent viscoelastic behavior of articular cartilage—the contributions from the intrinsic matrix viscoelasticity and interstitial fluid flows. J Biomech Eng 1986;108(2):123–30.
[56] Mak AF. Unconfined compression of hydrated viscoelastic tissues: a biphasic poroviscoelastic analysis. Biorheology 1986;23(4): 371–83.
[57] Suh JK, Bai S. Finite element formulation of biphasic poroviscoelastic model for articular cartilage. J Biomech Eng 1998;120(2): 195–201.
[58] Betsch DF, Baer E. Structure and mechanical properties of rat-tail tendon. Biorheology 1980;17:83–94.
[59] Haut RC. Age-dependent influence of strain rate on the tensile failure of rat-tail tendon. ASME J Biomech Eng 1983;105:296–9.
[60] Silver FH, Ebrahimi A, Snowhill PB. Viscoelastic properties of self-assembled type I collagen fibers: molecular basis of elastic and viscous behaviors. Connect Tiss Res 2002;43:569–80.
[61] Viidik Q. A rheological model for uncalcified parallel-fibriled collagenous soft tissue. J Biomech 1968;1:3–11.
[62] Wang JL, Parnianpour M, Shirazi-Adl A, Engin AE. Failure criterion of collagen fiber: viscoelastic behavior simulated by using load control data. Theoret Appl Fract Mech 1997;27:1–12.
[63] Haut RC, Little RW. A constitutive equation for collagen fibers. J Biomech 1972;5:423–30.
[64] Sanjeevi R, Somanathan N, Ramaswamy D. A viscoelastic model for collagen fibres. J Biomech 1982;15:181–3.
[65] Mow VC, Holmes MH, Lai WM. Fluid transport and mechanical properties of articular cartilage: a review. J Biomech 1984;17(5):377–94.
[66] Mow VC, Mak AF, Lai WM, Rosenberg LC, Tang LH. Viscoelastic properties of proteoglycan subunits and aggregates in varying solution concentrations. J Biomech 1984;17(5):325–38.
[67] Zhu W, Mow VC, Koob TJ, Eyre DR. Viscoelastic shear properties of articular cartilage and the effects of glycosidase treatments. J Orthop Res 1993;11(6):771–81.
[68] Mow VC, Kuei SC, Lai WM. Armstrong CG, biphasic creep and stress relaxation of articular cartilage in compression: theory and experiments. J Biomech Eng 1980;102:73–84.
[69] Lai WM, Mow VC. Drag-induced compression of articular cartilage during a permeation experiment. Biorheology 1980;17:111–23.
[70] Mow VC, Ratcliffe A. Structure and function of articular cartilage and meniscus. In: Mow VC, Hayes WC, editors. Basic orthopaedic biomechanics. 2nd ed. Philadelphia: Lippincott-Raven; 1997. p. 113–77.
[71] Holmes MH, Mow VC. The nonlinear characteristics of soft gels and hydrated connective tissues in ultrafiltration. J Biomech 1990;23:1145–56.
[72] Soltz MA, Ateshian GA. Experimental verification and theoretical prediction of cartilage interstitial fluid pressurization at an impermeable contact interface in confined compression. J Biomech 1998;31:927–34.
[73] Setton LA, Zhu W, Mow VC. The biphasic poroviscoelastic behavior of articular cartilage: role of the surface zone in governing the compressive behavior. J Biomech 1993;26(4/5):581–92.
[74] Gu WY, Lai WM, Mow VC. Transport of fluid and ions through a porous-permeable charged-hydrated tissue, and streaming potential data on normal bovine articular cartilage. J Biomech 1993;26:709–23.
[75] Gu WY, Lai WM, Mow VC. A mixture theory for charged-hydrated soft tissues containing multi-electrolytes: passive transport and swelling behaviors. J Biomech Eng 1998;120:169–80.
[76] Maroudas A. Transport of solutes through cartilage: permeability to large molecules. J Anat 1976;122:335–47.
[77] Lai WM, Hou JS, Mow VC. A triphasic theory for the swelling and deformation behaviours of articular cartilage. J Biomech Eng 1991;113:245–58.
[78] Bader DL, Kempson GE, Egan J, Gilbey W, Barrett AJ. The effects of selective matrix degradation on the short-term compressive properties of adult human articular cartilage. Biochim Biophys Acta 1992;1116(2):147–54.
[79] Huang C-H, Mow VC, Ateshian GA. The role of flow-independent viscoelasticity in the biphasic tensile and compressive responses of articular cartilage. J Biomech Eng 2001;123:410–7.
[80] Hayes WC, Bodine AJ. Flow-independent viscoelastic properties of articular cartilage matrix. J Biomech 1978;11(8–9):407–19.
[81] Spirt AA, Mak AF, Wassell RP. Nonlinear viscoelastic properties of articular cartilage in shear. J Orthop Res 1989;7(1):43–9.
[82] Wang CC, Guo XE, Sun D, Mow VC, Ateshian GA, Hung CT. The functional environment of chondrocytes within cartilage subjected to compressive loading: a theoretical and experimental approach. Biorheology 2002;39(1–2):11–25.
[83] Chen SS, Falcovitz YH, Schneiderman R, Maroudas A, Sah RL. Depth-dependent compressive properties of normal aged human femoral head articular cartilage: relationship to FCD. Osteoarthritis Cartilage 2001;9(6):561–9.
[84] Maroudas A. Physicochemical properties of cartilage in the light of ion exchange theory. Biophys J 1968;8(5):575–95.
[85] Akizuki S, Mow VC, Muller F, Pita JC, Howell DS. Tensile properties of human knee joint cartilage. II. Correlations between weight bearing and tissue pathology and the kinetics of swelling. J Orthop Res 1987;5:173–86.
[86] Adams ME. Cartilage hypertropy following canine anterior cruciate ligament transection differs among different areas of the joint. J Rheumatol 1989;16:818–24.
[87] Herzog W, Diet S, Suter E, Mayzus P, Leonard TR, Muller C, et al. Material and functional properties of articular cartilage and patellofemoral contact mechanics in an experimental model of osteoarthritis. Biomechanics 1998;31:1137–45.
[88] Setton LA, Mow VC, Muller FJ, Pita JC, Howel DS. Mechanical properties of canine articular cartilage are significantly altered following transection of the anterior cruciate ligament. Orthop Res 1994;12:451–63.
[89] Hoch DH, Grodzinsky AJ, Koob TJ, Albert ML, Eyre DR. Early changes in material properties of rabbit articular cartilage after meniscectomy. Orthop Res 1983;1:4–12.
[90] Jurvelin J, Kiviranta I, Arokoski J, Tammi M, Helminen HJ. Indentation study of the biomechanical properties of articular cartilage in the canine knee. Eng Med 1987;16:15–22.
[91] Dodge GR, Poole AR. Immunohistochemical detection and immunochemical analysis of type II collagen degradation in human normal, rheumatoid, and osteoarthritic articular cartilages and in explants of bovine articular cartilage cultured with interleukin 1. Clin Invest 1989;83:647–61.

[92] Haut RC, Ide TM, De Camp CE. Mechanical responses of the rabbit patello-femoral joint to blunt impact. J Biomech Eng 1995;117:402–8.
[93] Silyn-Roberts H, Broom ND. Fracture behaviour of cartilage-on-bone in response to repeated impact loading. Connect Tiss Res 1990;24:143–56.
[94] Repo R, Finlay J. Survival of articular cartilage after controlled impact. J Bone Joint Surg 1977;73A:990–1001.
[95] Tomatsu T, Imai N, Takeuchi N, Takahashi K, Kimura N. Experimentally produced fractures of articular cartilage and bone. The effects of shear forces on the pig knee. J Bone Joint Surg Br 1992;74:457–62.
[96] Armstrong CG, Mow V, Wirth C. Biomechanics of impact-induced microdamage to articular cartilage: a possible genesis for chondromalacia patella. In: Finerman G, editor. AAOS Symposium on Sports Medicine. St. Louis: The Knee C.V. Mosby Co.; 1985. p. 70–84.
[97] Atkinson P, Haut RC. Subfracture insult to the human cadaver patellofemoral joint produces occult injury. J Orthop Res 1995; 13:936–44.
[98] Thompson R, Oegema T, Lewis J, Wallace L. Osteoarthritic changes after acute transarticular load. J Bone Joint Surg 1991;73A:990–1001.
[99] Vener J, RC T, Lewis J, Oegema T. Subchondral damage after acute transarticular loading: an in vitro model of joint injury. J Orthop Res 1992;10:759–65.
[100] McDevitt C, Gilbertson E, Muir H. An experimental model of osteoarthritis; early morphological and biochemical changes. J Bone Joint Surg 1977;59B:24–35.
[101] Lark MW, Bayne EK, Flanagan J, Harper CF, Hoerrner LA, Hutchinson NI, et al. Inhibition of cartilage degradation and changes in physical properties induced by IL-1beta and retinoic acid using matrix metalloproteinase inhibitors. Arch Biochem Biophys 1997;344:404–12.
[102] Sandy JD, Lark MW. Proteolytic degradation of normal and osteoarthritic cartilage matrix. In: Brand KD, Doherty M, Lohmander LS, editors. Osteoarthritis. Oxford: Oxford University Press; 1998. p. 84–93.
[103] Radin EL, Ehrlich MG, Chernack R, Abernethy P, Paul IL, Rose RM. Effect of repetitive impulsive loading on the knee joints of rabbits. Clin Othop 1978;131:288–93.
[104] Pelletier JP, Martel-Palletier J, Altman RD, Ghandur (Mnaymneh) L, Hower DS, Woessner JF. Collagenolytic activity and collagen matric breakdown of the articular cartilage in de Pond-Nuki dog model of osteoarthritis. Arthritis Rheum 1983;26:866–74.
[105] Guilak F, Ratcliffe A, Lane N, Rosenwasser MP, Mow VC. Mechanical and biochemical changes in the superficial zone of articular cartilage in canine experimental osteoarthritis. J Orthop Res 1994;12:474–84.
[106] Clark JM, Simonian PT. Scanning electron microscopy of 'fibrillated' and 'malacic' human articular cartilage: technical considerations. Microsc Res Techn 1997;37:299–313.
[107] Verzijl N, DeGroot J, Zaken CB, Braun-Benjamin O, Maroudas A, Bank RA, et al. Crosslinking by advanced glycation end products increases the stiffness of the collagen network in human articular cartilage. Arthritis Rheum 2001;46:114–23.
[108] Bank RA, Soundry M, Maroudas A, Mizrahi J, TeKoppele JM. The increased swelling and instantaneous deformation of osteoarthritic cartilage is highly correlated with collagen degradation. Arthritis Rheum 2000;43:2202–10.
[109] Saxena RK, Sahay KB, Guha SK. Morphological changes in the bovine articular cartilage subjected to moderate and high loadings. Acta Anat 1991;142:152–7.
[110] Panula HE, Hyttinen MM, Arokoski JP, Langsjo TK, Pelttari A, Kiviranta I. Articular cartilage superficial zone collagen birefringence reduced and cartilage thickness increased before surface fibrillation in experimental osteoarthritis. Ann Rheum Dis 1998;57(4):237–45.
[111] Hwang WS, Li B, Jin LH, Ngo K, Schachar NS, Hughes GN. Collagen fibril structure of normal, aging and osteoarthritic cartilage. J Pathol 1992;167(4):425–33.
[112] Hong SP, Henderson CNR. Articular cartilage surface changes following immobilization of the rat knee joint. Proc R Soc Acta Anat 1996;157:27–40.
[113] Lewis JL, Johnson SL. Collagen architecture and failure processes in bovine patellar cartilage. J Anat 2001;199:483–92.
[114] Broom ND. An enzymatically induced structural transformation in articular cartilage. Arthritis Rheum 1988;31:210–8.
[115] Smith Jr GN, Brandt KD. Hypothesis: can type IX collagen "glue" together intersecting type II fibers in articular cartilage matrix? A proposed mechanism. J Rheumatol 1992;19(1):14–7.
[116] McCormack T, Mansour JM. Reduction in tensile strength of cartilage precedes surface damage under repeated compressive loading in vitro. J Biomech 1998;31:55–61.
[117] Broom ND. The altered biomechanical state of human femoral head osteoarthritic. Arthritis Rheum 1984;27(9):1028–39.
[118] Broom ND. Abnormal softening in articular cartilage: its relationship to the collagen framework. Arthritis Rheum 1982;25(10): 1209–16.
[119] Lafeber FP, van Roy H, Wilbrink B, Huber-Bruning O, Bijlsma JW. Human osteoarthritic cartilage is synthetically more active but in culture less vital than normal cartilage. J Rheumatol 1992;19: 123–9.
[120] Ryu J, Treadwell BV, Mankin HJ. Biochemical and metabolic abnormalities in normal and osteoarthritic human articular cartilage. Arthritis Rheum 1984;27:49–57.
[121] Teshima R, Treadwell BV, Trahan CA, Mankin HJ. Comparative rates of proteoglycan synthesis and size of PG's in normal and osteoarthritic chondrocytes. Arthritis Rheum 1983;26:1225–30.
[122] Carter DR. Mechanical loading history and skeletal biology. Biomechanics 1987;20:1095–109.
[123] Woessner JF, Howel DS. Joint cartilage degradation: basic and clinical aspects. New York: Marcel Dekker Inc.; 1993.
[124] Hollander AP, Heathfield TF, Webber C, Iwata Y, Bourne R, Rorabeck C, et al. Increased damage to type II collagen in osteoarthritic articular cartilage detected by a new immunoassay. Clin Invest 1994;93:1722–32.
[125] Hollander AP, Pidoux I, Reiner A, Rorabeck C, Bourne R, Poole AR. Damage to type II collagen in ageing and osteoarthritis starts at the articular surface, originates around chondrocytes and extends into the cartilage with progressive degeneration. Clin Invest 1995;96:2859–69.
[126] Moldovan F, Pelletier JP, Hambor J, Cloutier JM, Martel-Pelletier J. Collagenase-3 (matrix metalloprotease 13) is preferentially localized in the deep layer of human arthritic cartilage in situ: in vitro mimicking effect by transforming growth factor beta. Arthritis Rheum 1997;40(9):1653–61.
[127] Okada Y, Shinmei M, Tanaka O, Naka K, Kimura A, Nakanishi I, et al. Localization of matrix metalloproteinase-3 (stromelysin) in osteoarthritic cartilage and synovium. Lab Invest 1992;66(6):680–90.
[128] Reboul P, Pelletier JP, Tardif G, Cloutier JM, Martel-Pelletier J. The new collagenase, collagenase-3 is expressed and synthesized by human chondrocytes but not by synoviocytes. A role in osteoarthritis. J Clin Invest 1996;97(9):2011–9.
[129] Shlopov BV, Lie WR, Mainardi CL, Cole AA, Chubinskaya S, Hasty KA. Osteoarthritic lesions: involvement of three different collagenases. Arthritis Rheum 1997;40(11):2065–74.
[130] Meachim G, Collins DH. Cell counts of normal and osteoartrotic articular cartilage in relation to the uptake of sulphate ($^{35}SO_4$), in vitro. Ann Rheum 1962;21:45–50.
[131] Rothwell AG, Bentley G. Chondrocyte multiplication in osteoarthritic articular cartilage. J Bone Joint Surg Br 1973;5(3): 588–94.

[132] Lee DA, Bentley G, Archer CW. The control of cell division in articular chondrocytes. Osteoarthritis Cartilage 1993;1(2):137–46.
[133] Vignon E, Arlot M, Vignon G. Cellular density of the femur head cartilage in relation to age. Rev Rhum Mai Osteoartic 1976;43: 403–5.
[134] Repo RU, Finlay JB. Survival of articular cartilage after controlled impact. Bone Joint Surg [Am] 1977;59:1068–76.
[135] Lewis JL, Deloria LB, Oyen-Tiesma M, Thompson Jr RC, Ericson M, Oegema Jr TR. Cell death after cartilage impact occurs around matrix cracks. J Orthop Res 2003;21(5):881–7.
[136] Chen CT, Bhargava M, Lin PM, Torzilli PA. Time, stress, and location dependent chondrocyte death and collagen damage in cyclically loaded articular cartilage. J Orthop Res 2003;21(5):888–98.
[137] Borrelli Jr J, Ricci WM. Acute effects of cartilage impact. Clin Orthop 2004;423:33–9.
[138] Huyghe JM, Janssen JD. Quadriphasic theory of swelling incompressible porous media. Int J Eng Sci 1997;35:793–802.
[139] Wang CC, Hung CT, Mow VC. An analysis of the effects of depth-dependent aggregate modulus on articular cartilage stress-relaxation behavior in compression. J Biomech 2001;34(1):75–84.
[140] Chen AC, Bae WC, Schinagl RM, Sah RL. Depth- and strain-dependent mechanical and electromechanical properties of full-thickness bovine articular cartilage in confined compression. J Biomech 2001;34(1):1–12.
[141] Ateshian GA, Warden WH, Kim JJ, Grelsamer RP, Mow VC. Finite deformation biphasic material properties of bovine articular cartilage from confined compression experiments. J Biomech 1997;30(11–12):1157–64.
[142] Bursac PM, Obitz TW, Eisenberg SR, Stamenovic D. Confined and unconfined stress relaxation of cartilage: appropriateness of a transversely isotropic analysis. J Biomech 1999;32(10):1125–30.
[143] Armstrong CG, Lai WM, Mow VC. An analysis of the unconfined compression of articular cartilage. J Biomech Eng 1984; 106(2):165–73.
[144] Mak AF, Lai WM, Mow VC. Biphasic indentation of articular cartilage. I. Theoretical analysis. J Biomech 1987;20(7):703–14.
[145] Mow VC, Gibbs MC, Lai WM, Zhu WB, Athanasiou KA. Biphasic indentation of articular cartilage. II. A numerical algorithm and an experimental study. J Biomech 1989;22(8–9):853–61.
[146] Suh JK, Spilker RL. Indentation analysis of biphasic articular cartilage: nonlinear phenomena under finite deformation. J Biomech Eng 1994;116(1):1–9.
[147] Atkinson P, Haut RC. Subfracture insult to the human cadaver patellofemoral joint produces occult injury. J Orthop Res 1995;13:936–44.
[148] Garcia JJ, Aliero NJ, Haut RC. An approach for stress analysis of transversely isotropic biphasic cartilage under impact load. J Biomech Eng 1998;120:608–13.
[149] Wu JZ, Herzog W, Epstein M. Joint contact mechanics in the early stages of osteoarthritis. Med Eng Phys 2000;22(1):1–12.
[150] Froimson MI, Ratcliffe A, Gardner TR, Mow VC. Differences in patellofemoral joint cartilage material properties and their significance to the etiology of cartilage surface fibrillation. Osteoarthritis Cartilage 1997;5(6):377–86.
[151] Lai WM, Mow VC, Roth V. Effects of nonlinear strain-dependent permeability and rate of compression on the stress behavior of articular cartilage. J Biomech Eng 1981;103:61–6.
[152] van der Voet A. A comparison of finite element codes for the solution of biphasic poroelastic problems. Proc Inst Mech Eng [H] 1997;211:209–11.
[153] Rietbergen R, Huiskes R. Elastic constants of cancellous bone. In: Cowin SC, editor. Bone mechanics handbook. CRC Press; 2001.
[154] Donzelli PS, Spilker RL, Ateshian GA, Mow VC. Contact analysis of biphasic transversely isotropic cartilage layers and correlations with tissue failure. J Biomech 1999;32(10):1037–47.
[155] Soltz MA, Ateshian GA. A conewise linear elasticity mixture model for the analysis of tension-compression nonlinearity in articular cartilage. J Biomech Eng 2000;122(6):576–86.
[156] Khalsa PS, Eisenberg SR. Compressive behavior of articular cartilage is not completely explained by proteoglycan osmotic pressure. J Biomech 1997;30(6):589–94.
[157] Huang CY, Mow VC, Ateshian GA. The role of flow-independent viscoelasticity in the biphasic tensile and compressive responses of articular cartilage. J Biomech Eng 2001;123(5):410–7.
[158] Soulhat J, Buschmann MD, Shirazi-Adl A. A fibril-network-reinforced biphasic model of cartilage in unconfined compression. J Biomech Eng 1999;121(3):340–7.
[159] Li LP, Soulhat J, Buschmann MD, Shirazi-Adl A. Nonlinear analysis of cartilage in unconfined ramp compression using a fibril reinforced poroelastic model. Clin Biomech 1999;14(9):673–82.
[160] Li LP, Buschmann MD, Shirazi-Adl A. A fibril reinforced nonhomogeneous poroelastic model for articular cartilage: inhomogeneous response in unconfined compression. J Biomech 2000;33(12):1533–41.
[161] Li LP, Buschmann MD, Shirazi-Adl A. The asymmetry of transient response in compression versus release for cartilage in unconfined compression. J Biomech Eng 2001;123:519–22.
[162] Li LP, Shirazi-Adl A, Buschmann MD. Alterations in mechanical behaviour of articular cartilage due to changes in depth varying material properties—a nonhomogeneous poroelastic model study. Comput Meth Biomech Biomed Eng 2002;5(1):45–52.
[163] Li LP, Buschmann MD, Shirazi-Adl A. Strain-rate dependent stiffness of articular cartilage in unconfined compression. J Biomech Eng 2003;125(2):161–8.
[164] Li LP, Herzog W. Strain-rate dependence of cartilage stiffness in unconfined compression: the role of fibril reinforcement versus tissue volume change in fluid pressurization. J Biomech 2004;37(3):375–82.
[165] Wilson W, van Donkelaar CC, van Rietbergen C, Ito K, Huiskes R. Stresses in the local collagen network of articular cartilage: a poroviscoelastic fibril-reinforced finite element study. J Biomech 2004;37(3):357–66.
[166] Wilson W, van Donkelaar CC, van Rietbergen B, Huiskes R. A fibril-reinforced poroviscoelastic swelling model for articular cartilage. J Biomech, in press.
[167] Korhonen RK, Laasanen MS, Toyras J, Lappalainen R, Helminen HJ, Jurvelin JS. Fibril reinforced poroelastic model predicts specifically mechanical behavior of normal, proteoglycan depleted and collagen degraded articular cartilage. J Biomech 2003;36(9):1373–9.
[168] DiSilvestro MR, Suh JK. A cross-validation of the biphasic poroviscoelastic model of articular cartilage in unconfined compression, indentation, and confined compression. J Biomech 2001;34(4):519–25.
[169] DiSilvestro MR, Zhu Q, Wong M, Jurvelin JS, Suh JK. Biphasic poroviscoelastic simulation of the unconfined compression of articular cartilage. I. Simultaneous prediction of reaction force and lateral displacement. J Biomech Eng 2001;123(2):191–7.
[170] DiSilvestro MR, Zhu Q, Suh JK. Biphasic poroviscoelastic simulation of the unconfined compression of articular cartilage. II. Effect of variable strain rates. J Biomech Eng 2001;123(2):198–200.
[171] DiSilvestro MR, Suh JK. Biphasic poroviscoelastic characteristics of proteoglycan-depleted articular cartilage: simulation of degeneration. Ann Biomed Eng 2002;30(6):792–800.
[172] Huyghe JM, Janssen CF, van Donkelaar CC, Lanir Y. Measuring principles of frictional coefficients in cartilaginous tissues and its substitutes. Biorheology 2002;39:47–53.
[173] Frijns AJH, Huyghe JM, Janssen JD. A validation of the quadriphasic mixture theory for intervertebral disc tissue. Int J Eng Sci 1997;35:1419–29.
[174] Huyghe JM, Houben GB, Drost MR, van Donkelaar CC. An ionised/non-ionised dual porosity model of intervertebral disc tissue. Biomech Model Mechanobiol 2003;2(1):3–19.

[175] Sun DD, Leong KW. A nonlinear hyperelastic mixture theory model for anisotropy, transport, and swelling of annulus fibrosis. Ann Biomed Eng 2004;32(1):92–102.
[176] Lanir Y. Biorheology and fluid flux in swelling tissues. I. Bicomponent theory for small deformations, including concentration effects. Biorheology 1987;24(2):173–87.
[177] Wilson W, van Donkelaar CC, Huyghe JM. Comparison between mechano-electrochemical and biphasic swelling theories for soft hydrated tissues. J Biomech Eng 2005;127(1):158–65.
[178] Eisenberg SR, Grodzinsky AJ. The kinetics of chemically induced nonequilibrium swelling of articular cartilage and corneal stroma. J Biomech Eng 1987;109(1):79–89.
[179] Brown TD, Singerman RJ. Experimental determination of the linear biphasic constitutive coefficients of human fetal proximal femoral chondroepiphysis. J Biomech 1986;19:597–605.
[180] Suh J-K, DiSilvestro MR. Biphasic poroviscoelastic behavior of hydrated biological soft tissue. J Appl Mech 1999;66:528–35.
[181] Eberhardt AW, Lewis JL, Keer LM. Contact of layered elastic spheres as a model of joint contact: effect of tangential load and friction. J Biomech Eng 1991;113:107–8.
[182] Kelly PA, O'Conner JJ. Transmission of rapidly applied loads through articular cartilage. Part 1. Uncracked cartilage. Proc Inst Mech Eng 1996;210:27–37.
[183] Askew M, Mow V. The biomechanical function of the collagen fibril ultrastructure of articular cartilage. J Biomech 1978;100:105–15.
[184] Eberhardt AW, Keer LM, Lewis JL, Vithoontien V. An analytical model of joint contact. J Biomech Eng 1990;112:407–13.
[185] Ateshian GA, Lai WM, Zhu WB, Mow VC. An asymptotic solution for the contact of two biphasic cartilage layers. J Biomech 1994;27:1347–60.
[186] Wilson W, van Donkelaar CC, Ito K, van Rietbergen B, Huiskes R. Pathways of load-induced cartilage damage causing cartilage degeneration in the knee after meniscectomy. J Biomech 2003;36:845–51.
[187] Breuls RG, Sengers BG, Oomens CW, Bouten CV, Baaijens FP. Predicting local cell deformations in engineered tissue constructs: a multilevel finite element approach. J Biomech Eng 2002;124(2):198–207.
[188] Mow VC, Proctor CS, Kelly MA. Biomechanics of articular cartilage. In: Nordin M, Frankel VH, editors. Basic biomechanics of the mucoskeletal system. 2nd ed. Philadelphia, PA: Lea and Febiger; 1989. p. 31–57.
[189] Wilson W, van Donkelaar CC, van Rietbergen C, Ito K, Huiskes R. Erratum to "Stresses in the local collagen network of articular cartilage: a poroviscoelastic fibril re-inforced finite element study" [J. Biomech. 37 (2004) 357–366] and "A fibril-reinforced poroviscoelastic swelling model for articular cartilage" [J. Biomech. (2005) in press], submitted.